Formation and characterization of poly(acrlonitrile)/Chitosan composite ultrafiltration membranes

Musale, D.A.; Kumar, A.; Pleizier, G.

Publisher's version / Version de l'éditeur:

Journal of Membrane Science, 154, pp. 163-173, 1999

ELSEVIER

Journal of Membrane Science 154 (1999) 163–173

journal of MEMBRANE SCIENCE

Formation and characterization of poly(acrylonitrile)/Chitosan composite ultrafiltration membranes

D.A. Musale, A. Kumar*, G. Pleizier

Institute for Chemical Process and Environmental Technology, National Research Council Canada, M-12, Montreal Road, Ottawa, Ont., Canada K1A 0R6

Received 15 May 1998; received in revised form 25 August 1998; accepted 25 August 1998

Abstract

The Poly(acrylonitrile) (PAN)/Chitosan composite ultrafiltration membranes were prepared by filtration of Chitosan solution through PAN base membrane and subsequent curing and treatment with NaOH. The formation of Chitosan layer on the surface as well as pore walls of PAN base membrane was characterized by different techniques. Fourier transform infrared-attenuated total reflectance, X-ray photoelectron spectroscopy and scanning electron microscopy studies indicated the formation of Chitosan layer on the surface, whereas determination of pure water permeation, pore size distribution and molecular weight cut off indicated the reduction in pore size due to formation of Chitosan layer on the pore walls of PAN base membrane. It was further observed that these composite membranes had sharper molecular weight cut off as well as narrower pore size distribution than the corresponding base membrane. The reduction in negative zeta potential of PAN base membrane at pH 9.0 and observation of positive zeta potential at pH 5.0 with composite membranes also confirmed the formation of Chitosan layer on the pore walls of base membrane. The composite membranes were found to be stable in aqueous medium and showed reduction in pure water fluxes measured after filtration of aqueous acidic (pH 3.0) and basic (pH 11.0) solution, which was attributed to the swelling of Chitosan layer.

Keywords: Composite membranes; Ultrafiltration; Membrane preparation and structure; Membrane potentials; Poly(acrylonitrile); Chitosan

1. Introduction

Chitosan is a biopolymer derived from Chitin and has found many applications in food, biotechnology and pharmaceutical industries as well as in medicine [1]. Chitosan based membranes have been used in reverse osmosis [2], gas separation [3], dialysis [4] and pervaporation [5–7]. It is used as a composite [6,8], polyelectrolyte complex [9,10] or a blend [11,12] with another polymer.

A recent review [13] has emphasized that in addition to the size exclusion mechanism, ultrafiltration process is governed by solute–solute and solute–membrane interactions that are dependent on membrane surface characteristics such as hydrophilic/hydrophobic balance and electrostatic charges on both membranes as well as solutes. The solute–membrane interactions are important on both membrane surface as well as membrane pore walls with which solute

*Corresponding author. Tel.: +1-613-998-0498; fax: +1-613-941-2529; e-mail: ashwani.kumar@nrc.ca

0376-7388/99/$ – see front matter
PII: S0376-7388(98)00265-8

molecules come in contact during filtration. The hydrophilicity of membrane material plays an important role in reducing fouling and hence maintaining permeate fluxes [14,15]. It has also been reported that an increase in hydrophilicity of membrane material results in increasing protein transmission [15]. Furthermore, higher permeate fluxes [16] and higher protein rejections [17] have been observed for membranes and proteins having similar charges (either positive or negative). Chitosan is a hydrophilic material and likely to impart the hydrophilicity to the membranes prepared by formation of its composite with another mechanically stronger and hydrophobic material such as poly(acrylonitrile) (PAN). In acidic pH range, Chitosan will be positively charged due to protonation of $-NH_2$ groups and hence will exhibit the electrostatic interactions with charged solutes such as proteins. Application of Chitosan for ultrafiltration membranes has been reported by Aiba et al. [18], Kaminski and Modrzejewska [19] and Wang and Spencer [20]. To our knowledge there is no reported literature on PAN/Chitosan composite ultrafiltration membranes, although studies on PAN/Chitosan composite pervaporation membranes are reported [5,6]. Therefore, it will be interesting to investigate the formation of composite ultrafiltration membranes utilizing the unique properties of PAN and Chitosan.

The present study reports the formation of PAN/Chitosan composite ultrafiltration membranes and characterization of Chitosan layer on the surface as well as on the pore walls of PAN base membrane, including pure water permeation, molecular weight cut off, pore size distribution and zeta potential measurements.

2. Experimental

2.1. Materials

Poly(acrylonitrile) (PAN) (MW 1.5×10^5 Da) and Chitosan were procured from Polysciences, USA. Chitosan was purified by dissolving in aqueous (aq.) acetic acid (2% w/w) and precipitating in 4% aq. sodium hydroxide. The molecular weight of Chitosan was 1.16×10^5 Da as determined from measured intrinsic viscosity [η] in a buffer solvent system (0.3 M acetic acid and 0.2 M sodium acetate) at 25°C and Mark-Houwink constants ($K=7.4\times10^{-4}$ dl g^{-1} and $a=0.76$), using Mark-Houwink–Sakurda equation ($[\eta]=KM^a$). The constants K and a, were the literature values [21] obtained from the double logarithmic plot of intrinsic viscosity versus molecular weight of polymer and are functions of solvent and polymer types. The degree of deacetylation of Chitosan as determined from ^{1}H-NMR (Varian, 400 MHz) in D_2O in presence of CD_3COOD using the integrals of $-CH_3$ and H-2 (as an internal standard) [21] was found to be about 86%.

Polyethylene glycols, Dextran and Polyethylene oxides were obtained from Aldrich, or Polysciences. All other reagents were obtained from Anachemia, Canada and used as received. Reverse osmosis treated water with conductivity of 5×10^{-4} S m^{-1} was used throughout this study.

2.2. Preparation of base membrane (PAN)

The base membrane was prepared by casting *N*,*N*-dimethyl formamide (DMF) solution of PAN (9% w/w) on non-woven porous polyester support (Hollytex 3329) at a casting speed of 0.068 m s^{-1} and subsequent gelation in water at 20°C. The relative humidity of the casting environment was 17%. The cast membrane was then washed overnight with water before use.

2.3. Preparation of PAN/Chitosan composite UF membrane (PANCHIUF)

The PAN/Chitosan composite membranes were prepared by filtering the Chitosan solution (0.5% w/w) in aq. acetic acid (2% w/w) through the PAN base membrane at 200 kPa for 10 s using stirred cell assembly (Amicon, 28.7×10^{-4} m^2 area, 600 rpm). This was followed by curing the membranes at 60°C for 15 min. This Chitosan acetate composite layer was then converted to Chitosan by filtering NaOH (1 M in ethanol–water mixture, 1:1) through the cured membranes for 3 min under similar pressure and stirring conditions. These membranes were subsequently washed with ethanol–water mixture (1:1) to remove NaOH, by filtering it through the membrane for 2 min under similar experimental conditions. The procedure of curing the membranes at 60°C and washing with

ethanol–water mixture was similar to the description outlined in [5,22]. These PAN/Chitosan composite membranes (PANCHIUF) were then washed overnight in running water before further characterization.

In order to verify the effect of acetic acid and sodium hydroxide treatment on base membrane surface characteristics, the base membrane was treated under similar conditions as above without the presence of Chitosan in acetic acid solution. These membranes are designated as PANCHIUF-B.

2.4. Membrane characterization

The formation of composite Chitosan layer was characterized on the membrane surface as well as on the pore walls.

2.4.1. Surface characterization

The composite layer of Chitosan on PAN microporous membrane surface was characterized by Fourier transform infrared–attenuated total reflectance (FTIR–ATR), scanning electron microscopy (SEM) and X-ray photoelectron spectroscopy (XPS).

2.4.1.1. FTIR–ATR. FTIR–ATR studies were done on vacuum dried membrane samples using ZnSe crystal with Nicolet-520 FTIR Spectrometer. The spectra were taken at an incidence angle of 45° with 50 scans at a resolution of 4 cm^{-1}. The Chitosan membrane was prepared by casting 3% (w/w) solution of Chitosan in 0.3 M acetic acid and 0.2 M sodium acetate on glass plate and precipitating in a solution containing 4% NaOH in ethanol–water mixture (1:1). It was then washed several times with water; air dried and finally vacuum dried at 40°C for seven days.

2.4.1.2. XPS. XPS studies on vacuum dried membrane samples were carried out with Kratos axis X-ray photoelectron spectrometer using monochromated Al K_α X-radiation and charge neutralization. Same Chitosan membrane sample was used as that for FTIR–ATR studies. The spectrometer was operated in fixed analyzer transmission (FAT) mode using electrostatic magnification. High resolution spectra were collected using 40 eV pass energy. Each sample was analyzed at two locations and the data presented is the average of two values.

2.4.1.3. SEM. SEM studies were carried out on gold sputtered (one minute) membrane samples using Jeol (JSM 5300) scanning electron microscope at an accelerating voltage of 10 kV. Membrane samples for SEM studies were prepared by soaking in isopropanol overnight, then in hexane for 10 h and subsequent vacuum drying at 40°C for three days. The cross-sections of samples were prepared by fracturing in liquid nitrogen.

2.4.2. Pore size related characterization

2.4.2.1. Pure water permeation (PWP). The pure water permeation was measured with all membranes using the same stirred cell assembly mentioned previously, at 200 kPa and 600 rpm.

2.4.2.2. Pore size distribution. The pore size distribution of all membrane samples was determined by modified bubble point method as described in [23]. In brief, water saturated *i*-butanol (σ=1.7 dynes cm^{-1}) was used to displace water in prewetted membranes with constant increment of pressure. The pore radii (r_{pj}) and the number of pores were determined using Cantor's relation (Eq. (1)) and Hagen-Poiseuille's equation (Eq. (2)), respectively:

$$r_{pj} = \frac{2\sigma\cos\theta}{P_j}, \tag{1}$$

$$n_j = \left[Q_j - \frac{Q_{j-1}P_j}{P_{j-1}}\right]\frac{8\eta d}{\pi P_j r_{pj}^4}, \tag{2}$$

where σ, θ, n, η, d, P and Q are the water/water saturated *i*-butanol interfacial tension, water/polymer contact angle, number of pores, viscosity, pore length (membrane skin layer thickness), applied pressure and the permeate flow rate, respectively.

2.4.2.3. Molecular weight cut off (MWCO). Molecular weight cut offs of all membrane samples were measured using 0.1% (w/w) solutes such as polyethylene glycols (PEG) (MW 10, 20 and 35 kD), Dextran (42 and 75 kD) and polyethylene oxides (PEO) (100, 200 and 300 kD) in water. The concentrations of these test solutes in feed and permeate samples were determined by Shimadzu 5000 Total Organic Carbon analyzer.

2.4.3. Zeta potential measurements

In order to study the pore wall characteristics, zeta potentials (ζ) of all membranes were measured by electro-osmosis method at pH 5.0 and 9.0. The details of the method are reported elsewhere [24]. Zeta potentials were calculated from the electro-osmotic flow rate using Smoluchowski relationship [24] given below:

$$\zeta = \frac{V\eta k}{I\epsilon}, \tag{3}$$

where V, η, k, ϵ, and I are the electro-osmotic flow rate, viscosity, specific conductivity, permittivity of electrolyte solution and the applied current, respectively.

3. Results and discussion

The Chitosan layer was deposited on the surface as well as on pore walls of PAN base membrane. This resulted in the reduction of pore size of base membrane and an increase in hydrophilicity. The extent of pore size reduction will depend on the experimental conditions of composite membrane formation, such as filtration time and concentration of the Chitosan solution. Wang and Spencer [20] have reported the formation of Chitosan on titanium dioxide macroporous substrate. However, these membranes were dynamic in nature while the present work reports the formation of composite membranes. The schematic of composite membrane formation is shown in Fig. 1. Furthermore, there is no literature reference on Chitosan composite membranes on PAN base using this procedure. Modification of surface chemistry of membrane pore walls is important in many ultrafiltration applications, where various solute–membrane interactions determine the membrane performance [13].

3.1. Surface characterization

3.1.1. FTIR–ATR

The FTIR–ATR technique has been used previously for the characterization of membrane surfaces [25,26]. Figs. 2 and 3 show the FTIR–ATR spectra for PAN, Chitosan, PANCHIUF-B and PANCHIUF membranes in the regions 1800–800 cm^{-1} and 3800–2000 cm^{-1}, respectively. It is clear from Figs. 2 and 3 that new bands at 1725 cm^{-1} and 3275 cm^{-1} are observable for PANCHIUF-B membranes compared to PAN membranes. These new bands are attributed respectively to the >C=O and –O–H stretching frequencies of carboxylic acid groups formed due to slight hydrolysis of nitrile groups of base membrane by NaOH. In case of Chitosan and PANCHIUF membranes, the bands at 1650 (amide I) and 1590 cm^{-1} (Fig. 2) are characteristic of >C=O stretching of *N*-acetyl group and –N–H deformation in amino group, respectively. Also, the band at 900 cm^{-1} in the case of Chitosan and PANCHIUF membranes is characteristic of –N–H wagging frequency. The bands at 1030 cm^{-1} in Chitosan and 1050 cm^{-1} in PANCHIUF (Fig. 2) are attributed to –C–O stretching in cyclic alcohols. The –C–O–C stretching, characteristic of ether linkage is seen in case of Chitosan and PANCHIUF membranes at 1150 cm^{-1} (Fig. 2).

Fig. 3 shows the bands at 2240 cm^{-1} (–C≡N stretching) in case of PAN and PANCHIUF-B and –N–H stretching (at 3370 cm^{-1} in $–NH_2$ and 3270 cm^{-1} in $–NHCOCH_3$) and –O–H stretching at 3450 cm^{-1} in case of Chitosan and PANCHIUF membranes. The band at 2870 cm^{-1} in Chitosan and PANCHIUF membranes is due to –C–H stretching in $–NHCOCH_3$ group. The presence of band at 2240 cm^{-1} in PANCHIUF membranes is due to the exposure of PAN base membrane to the IR radiation.

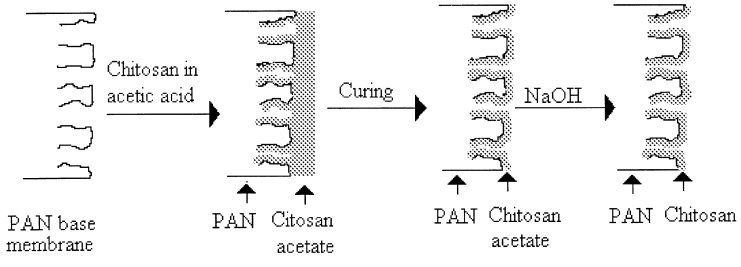

Fig. 1. A schematic of composite ultrafiltration membrane formation.

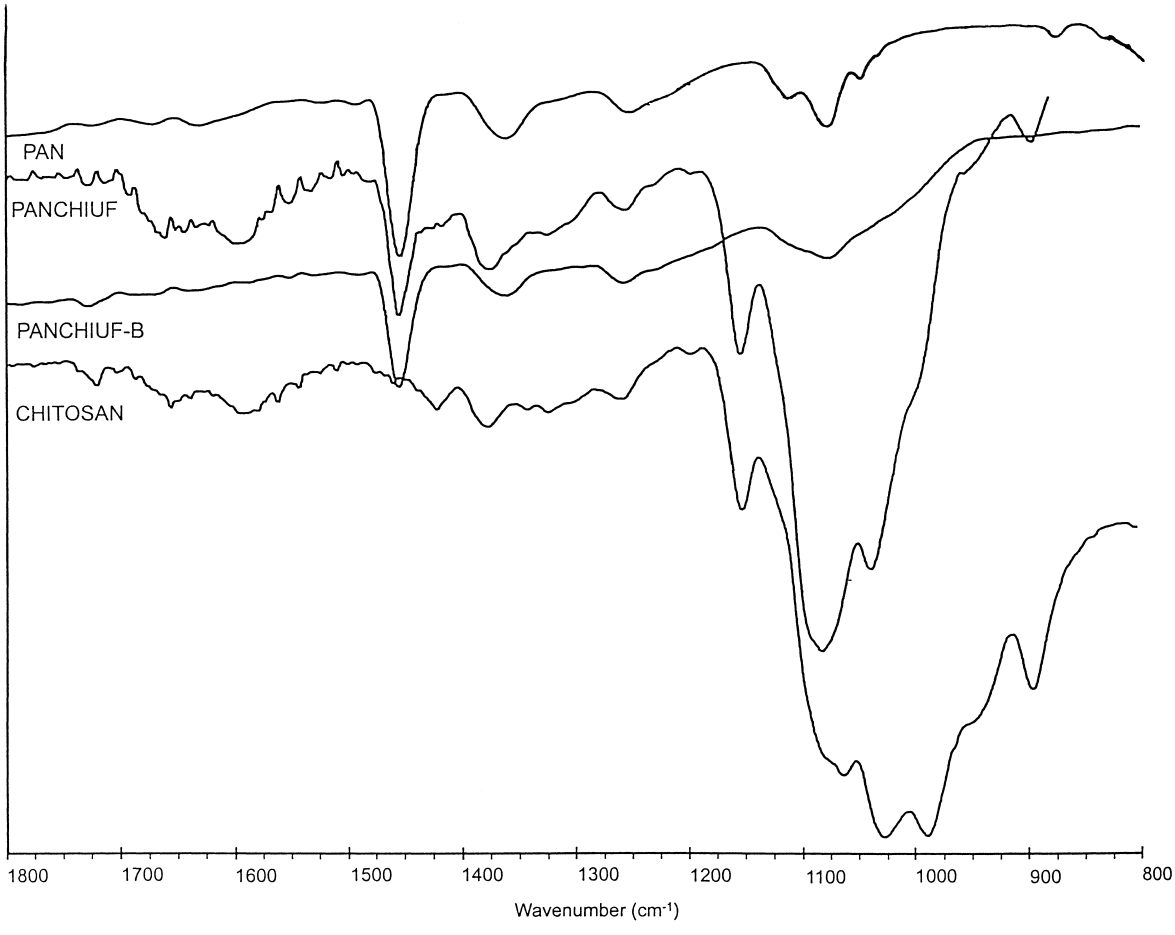

Fig. 2. FTIR–ATR spectra of PAN, PANCHIUF-B, CHITOSAN and PANCHIUF membranes in the region 1800–800 cm^{-1}.

In order to explain this conclusion, the penetration depth (d_p) was calculated at different wavelengths (λ) as described in [27]:

$$d_p = \frac{\lambda}{2\pi[n_1^2 \sin^2\theta - n_2^2]^{1/2}}, \quad (4)$$

where n_1, n_2 and θ are refractive indices of ZnSe crystal, Chitosan and angle of incidence of IR radiation, respectively. The refractive index of Chitosan was measured on transparent membrane (same as used for FTIR and XPS studies) using Abbe C10 refractometer and was found to be 1.6575. The penetration depths calculated at 1000, 1600, 2000, 2240, 2900 and 3400 cm^{-1} were 4.36, 2.73, 2.18, 1.95, 1.5 and 1.28 μm, respectively. It is clear from these data that IR beam reaches deeper near nitrile group region (2240 cm^{-1}) beyond the Chitosan layer which is significantly smaller than d_p as seen in SEM studies described later. For the similar reason, the band at 1455 cm^{-1} (Fig. 2) that is characteristic of $-CH_2$ scissors vibration is observed in PANCHIUF membranes similar to those seen in PAN and PANCHIUF-B membranes. Thus, in addition to bands characteristic of Chitosan, the bands at 2240 and 1455 cm^{-1} due to PAN are also seen in case of PANCHIUF membranes. All of the above observations clearly reveal the presence of Chitosan layer in case of PANCHIUF membranes.

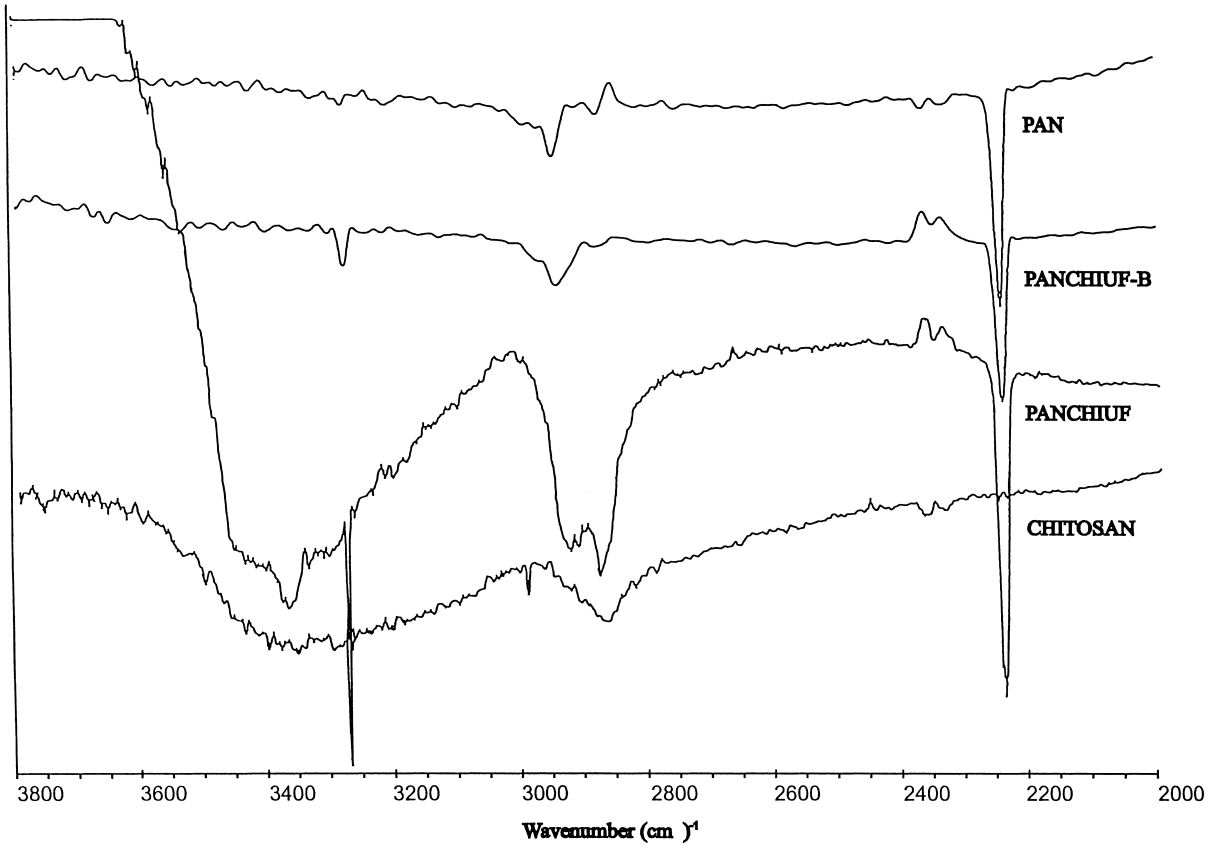

Fig. 3. FTIR–ATR spectra of PAN, PANCHIUF-B, CHITOSAN and PANCHIUF membranes in the region 3800–2000 cm^{-1}.

3.1.2. XPS

The atomic composition (%) of surfaces of PAN, Chitosan, PANCHIUF-B and PANCHIUF membranes determined by XPS are shown in Table 1. It is clear from Table 1 that the concentrations of C, N and O in PANCHIUF membranes agree well with those of Chitosan membrane. Also, the C/O and C/N ratios of PANCHIUF are comparable with those of Chitosan. These observations confirm the formation of Chitosan layer on PAN base membrane. A decrease in C/O ratio in PANCHIUF-B compared to that in PAN is indicative of the slight hydrolysis of nitrile groups of PAN to carboxylic acid by NaOH.

3.1.3. SEM

Scanning electron micrographs of surfaces and cross-sections of PAN, PANCHIUF-B and PANCHIUF membranes are shown in Figs. 4 and 5,

Table 1
Atomic composition (%) of surfaces of different membranes measured by XPS

Membrane	Carbon (C)	Oxygen (O)	Nitrogen (N)	C/O	C/N
PAN	75.8	2.1	22.1	36.09	3.42
PANCHIUF-B	73.4	4.6	21.2	15.95	3.46
PANCHIUF	61.5	29.9	8.6	2.05	7.15
CHITOSAN	60.3	32.0	7.7	1.88	7.83

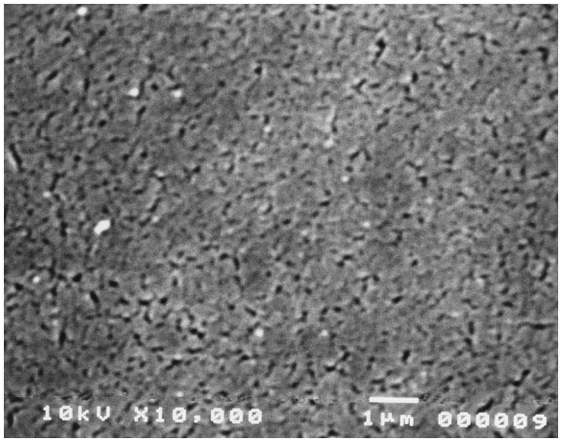

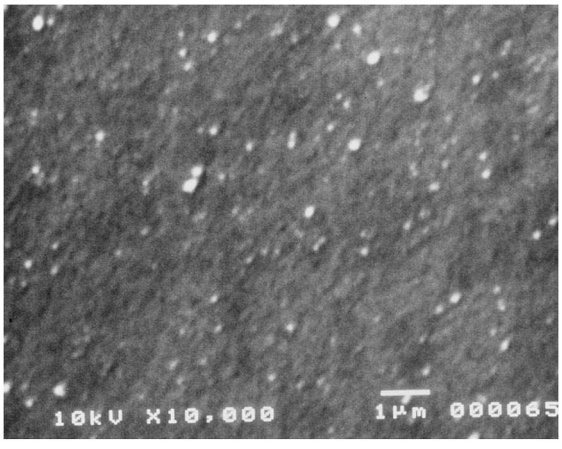

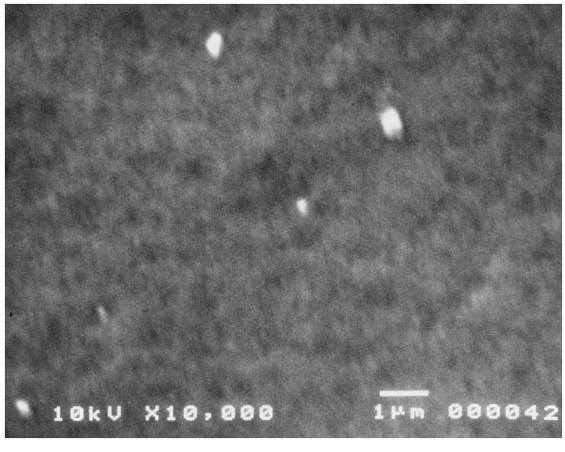

Fig. 4. Scanning electron micrographs of surfaces of: (a) PAN, (b) PANCHIUF-B and (c) PANCHIUF membranes.

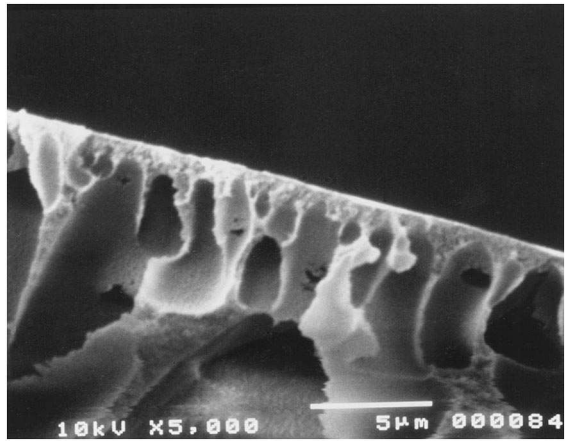

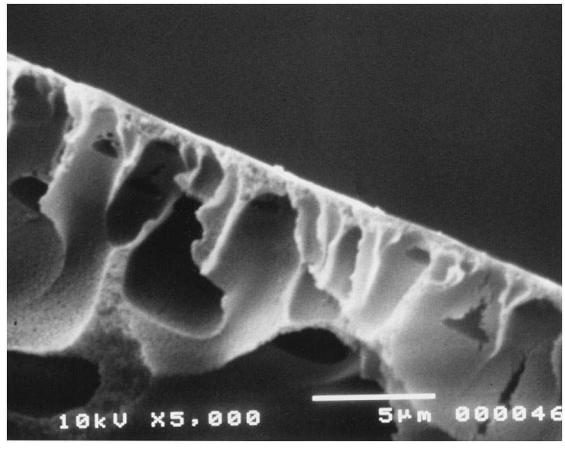

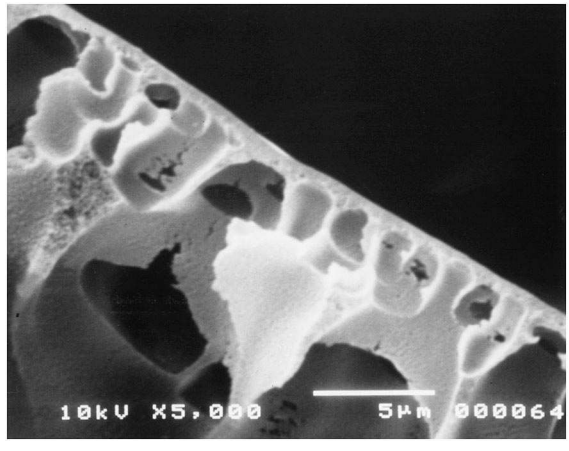

Fig. 5. Scanning electron micrographs of cross-sections of: (a) PAN, (b) PANCHIUF-B and (c) PANCHIUF membranes.

respectively. As can be seen from Fig. 4, the base membrane (PAN) clearly shows the presence of pores on membrane surface (Fig. 4(a)), while in the case of PANCHIUF membranes (Fig. 4(c)) the pore openings are covered. However, the coated Chitosan layer is so thin that the pore openings of the base membrane are only partially visible. Fig. 4(b) shows that there is a slight change in the surface morphology of base membrane with the blank solution (the solution without Chitosan) treatment. This may be attributed to slight hydrolysis of nitrile groups to carboxylic acid on the base membrane by NaOH that is shown by FTIR–ATR and XPS studies (Figs. 2 and 3 and Table 1) also. Therefore it can be concluded that the surface of the base membrane is covered by a thin layer of Chitosan. However, the thickness of Chitosan layer in PANCHIUF membranes (Fig. 5(c)) is too small to be detected on top of the skin of asymmetric structure of PAN membrane (Fig. 5(a)). Fig. 5(b) shows that the blank solution treatment does not affect the pore tortuosity of the base membrane.

3.2. Pore size related characterization

3.2.1. Pure water permeation

Table 2 shows the average pure water fluxes measured on four samples of each membrane. It is clear from Table 2 that the pure water flux of base membrane was reduced to 5% of initial water flux after 10 s of filtration with Chitosan solution followed by subsequent treatment. The reduction of pure water flux in case of PANCHIUF-B membrane compared to PAN membrane may be attributed to the collapse of some pores at 60°C as PAN membranes are reported to have an operation temperature limit of 60°C [28].

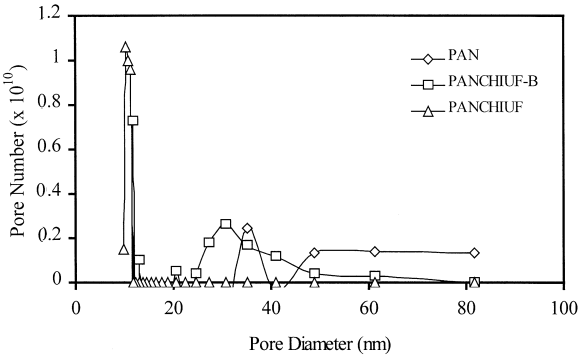

Fig. 6. Pore size distribution for PAN (◇), PANCHIUF-B (□) and PANCHIUF (△) membranes.

3.2.2. Pore size distribution

The coating of Chitosan on pore walls of PAN membrane is expected to reduce the pore size of base membrane. Fig. 6 shows the typical pore size distribution for PAN, PANCHIUF-B and PANCHIUF membranes and mode pore size for the corresponding membranes is shown in Table 2. As can be seen from Fig. 6, in case of PANCHIUF membranes all larger diameter (>30 nm) pores present in the microporous base membrane (PAN) are reduced in size as well as in number. The base membrane has most of the pores of diameter >30 nm, while PANCHIUF has maximum pores of the mode pore size of ≈10 nm. These observations clearly indicate the formation of Chitosan layer on the pore walls of the base membrane. There is a reduction in larger sized pores in PANCHIUF-B membranes also, which may be attributed to the curing temperature effect as mentioned above. However, this reduction in pore size is not significant.

3.2.3. Molecular weight cut off

The formation of Chitosan layer on the pore walls of base membrane was also confirmed by the determina-

Table 2
Pore size related membrane characteristics

Membrane	Pure water flux ($l\,m^{-2}\,h^{-1}$)[a]	Mode pore size (nm)[b]	Molecular weight cut off (kD)[c]
PAN	4000±100	≥35	>300
PANCHIUF-B	1800±100	30	>300
PANCHIUF	200±20	10	75

[a]Measured at 200 kPa and 600 rpm.
[b]Measured using modified bubble point method.
[c]Measured using PEG, PEO and dextran as test solutes.

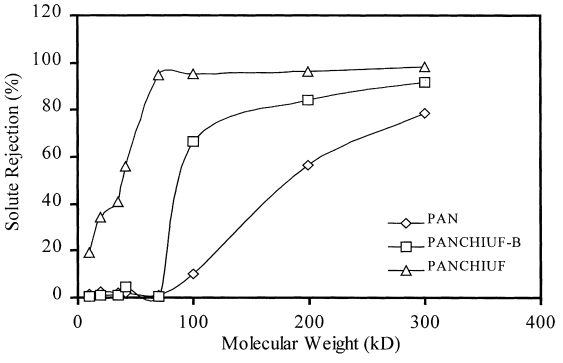

Fig. 7. Average molecular weight cut offs for PAN (◇), PANCHIUF-B (□) and PANCHIUF (△) membranes.

tion of the molecular weight cut offs of all membrane samples using polyethylene glycols (PEG), Dextran and polyethylene oxides (PEO) as test solutes. These data are shown as the average of two measurements in Fig. 7. These data were reproducible to ±9%. Fig. 7 shows that, the MWCO of the base membrane (>300 kD) is reduced to 75 kD in case of PANCHIUF membranes. The MWCO of PANCHIUF-B membranes is also slightly reduced in comparison to base membrane, which is consistent with the reduction in pure water flux and mode pore size. Thus, the MWCO of PAN membrane was reduced by a factor of ≈5 due to the formation of Chitosan layer on the pore walls of PAN membrane. Interestingly, the MWCO curve of PANCHIUF membranes is sharper than that of PAN. This observation also supports the conclusion of reduction in large sized pores due to formation of Chitosan layers on pore walls of PAN base membrane.

3.3. Zeta potential studies

The average zeta potential values of the two measurements for PAN, PANCHIUF-B and PANCHIUF membranes at pH 5.0 and 9.0 are shown in Table 3. The measurements were reproducible to ±22%. As expected, PAN membrane is negatively charged at both pH values, which is consistent with the previous study [15]. Table 3 shows that the zeta potential of PANCHIUF membranes is lower than that of PAN at pH 9.0. This reduction in negative charge is explained as follows. The zeta potential of polymeric membranes arises partly due to adsorption of ions from the polar medium such as aq. KCl solution in the present case. Chitosan is known to be more hydrophilic than PAN, therefore adsorption of anions from the solution on Chitosan layer of PANCHIUF membranes is lower, which resulted in reduced negative charge on Chitosan layer at pH 9.0. At pH 5.0, the positive zeta potential of PANCHIUF membranes is attributed to the protonation of $-NH_2$ groups in Chitosan layer. The increase in negative zeta potential in case of PANCHIUF-B membrane in comparison to PAN at both pH values, may be attributed to the presence of negatively charged carboxylate ions formed due to slight hydrolysis of PAN by NaOH. This reduction in negative zeta potential at pH 9.0 and exhibition of positive zeta potential at pH 5.0 in the case of PANCHIUF membranes while the measurements are made through the pores, confirm the formation of Chitosan layer on the pore walls of the base membrane.

Table 3
Zeta potentials for PAN, PANCHIUF-B and PANCHIUF membranes at pH 5.0 and pH 9.0

Membrane	Zeta potential (mV)	
	pH 5.0	pH 9.0
PAN	−19.4	−21.6
PANCHIUF-B	−30.2	−39.0
PANCHIUF	10.4	−13.0

3.4. Stability of Chitosan layer in aqueous medium

In order to verify the integrity of Chitosan membrane with PAN, PANCHIUF membranes were washed for 10 days in running water and the pure water flux was measured at 200 kPa and 600 rpm everyday. It was observed that, the pure water flux remained constant over this period of measurement (Table 2) which indicates that the Chitosan layer is adhering very well to the base membrane and stable in aqueous medium. The integrity was also tested at pH 3.0 and 11.0 by filtering aq. acidic and basic solutions, respectively, through PANCHIUF membranes at 200 kPa and 600 rpm for 1 h. It was observed that, the pure water fluxes measured after the filtration of both acidic and basic solutions were reduced to ≈60% of water flux measured before pH treatment. This may be attributed to the reduction in pore size due to increased swelling of Chitosan, which in turn may

be attributed to protonation of $–NH_2$ groups at pH 3.0 and $–NH^-$ group formation at pH 11.0. Thus, expansion of polymer chains due to electrostatic repulsion in Chitosan resulted in increased swelling and hence the reduction in pore sizes. The reduction in pore size of Chitosan membrane at pH 3.6 is also observed by Wang and Spencer [20].

It is evident from all characterization results that a stable Chitosan layer can be formed on PAN microporous support to make an ultrafiltration membrane. Although the NaOH treatment was performed on the Chitosan acetate layer in the case of PANCHIUF membrane preparation, it is likely that NaOH might have diffused through the Chitosan layer and hydrolyzed some nitrile groups to carboxylic acid groups. Subsequently, $–NH_2$ of Chitosan might react with these newly formed –COOH groups of PAN and form –CONH-bonding between the two polymers. The formation of such amide bonding in PAN/Chitosan system is also suggested by Wang et al. [6]. Since Chitosan also has amide functionality in its molecular chain, these newly formed amide bonds cannot be distinguished in IR spectra. The XPS technique is applicable only to top 4–7 nm thick layer, therefore C/O ratio in PANCHIUF was same as that of Chitosan and was not reduced due to this new oxygen. However, the decrease in C/O ratio was observable in PANCHIUF-B compared to PAN, which indicates the hydrolysis of nitrile groups.

4. Conclusions

1. The Poly(acrylonitrile) (PAN)/Chitosan composite ultrafiltration membranes were prepared by filtration of Chitosan solution through PAN base membrane and subsequent curing and treatment with NaOH.
2. FTIR–ATR and XPS studies indicated the presence of functional groups that are characteristic of Chitosan on the surface of the composite membranes. SEM studies revealed the presence of very thin coating of Chitosan on PAN.
3. Pure water permeation, pore size distribution and molecular weight cut off results indicated the reduction in pore size due to formation of Chitosan layer on the pore walls of PAN base membrane. In composite membranes, the molecular weight cut off was sharper and pore size distribution was narrower than the base membrane.
4. The reduction in negative zeta potential at pH 9.0 and exhibition of positive zeta potential at pH 5.0 in composite membranes also confirmed the formation of Chitosan layer on the pore walls of base membrane.
5. The treatment of PAN membrane with acetic acid and subsequently NaOH solution showed slight hydrolysis of nitrile groups to carboxylic acid groups. Therefore, the formation of composite layer of Chitosan may be through amide bonding between $–NH_2$ of Chitosan and newly formed carboxylic acid groups of PAN.
6. The composite ultrafiltration membranes were found to be stable in aqueous medium, while the pure water fluxes measured after aqueous acidic (pH 3.0) and aqueous basic (pH 11.0) solution treatment were reduced due to increased swelling of Chitosan.

Acknowledgements

Authors are grateful to M.M. Dal-Cin for base membrane casting on automated casting machine and G. Robertson for NMR spectra of Chitosan.

References

[1] M.F.A. Goosen (Ed.), Applications of Chitin and Chitosan, Technomic Publishing, Lancaster, 1997.
[2] T. Yang, R.R. Zall, Chitosan membranes for reverse osmosis application, J. Food Sci. 49 (1984) 91.
[3] Y. Mizushima, Preparation of alkoxide-derived Chitosan-silica complex membrane, J. Non-Cryst. Solids 144 (1992) 305.
[4] S. Hirano, K. Tobetto, M. Hasegawa, N. Matsuda, Permeability properties of gels and membranes derived from Chitosan, J. Biomed. Mat. Res. 14 (1980) 477.
[5] K. Watanabe, S. Kyo, Pervaporation performance of hollow-fibre Chitosan/poly(acrylonitrile) composite membrane in dehydration of ethanol, J. Chem. Eng. Jpn. 25(1) (1992) 17.
[6] X.P. Wang, Z.Q. Shen, F.Y. Zhang, Y.F. Zhang, A novel composite Chitosan membrane for the separation of alcohol–water mixtures, J. Membr. Sci. 119 (1996) 191.
[7] X. Feng, R.Y.M. Huang, Pervaporation with Chitosan membranes. I. Separation of water from ethylene glycol by a Chitosan/polysulfone composite membrane, J. Membr. Sci. 116 (1996) 67.

[8] M.G.M. Nawawi, R.Y.M. Huang, Pervaporation dehydration of isopropanol with Chitosan membranes, J. Membr. Sci. 124 (1997) 53.
[9] C. Peniche-Covas, W. Argüelles-Monal, J.S. Román, Sorption and desorption of water vapour by membranes of the polyelectrolyte complex of Chitosan and carboxymethyl cellulose, Polym. Int. 38 (1995) 45.
[10] E.P. Ageev, S.L. Kotova, E.E. Skorikova, A.B. Zezin, Pervaporation membranes based on polyelectrolyte complexes of Chitosan and poly(acrylic acid), Polym. Sci. Ser. A 38(2) (1996) 202.
[11] M.M. Amiji, Permeability and blood compatibility properties of Chitosan poly(ethylene oxide) blend membranes for haemodialysis, Biomaterials 16 (1995) 593.
[12] J.J. Shieh, R.Y.M. Huang, Pervaporation with Chitosan membranes. II. Blend membranes of Chitosan and poly(-acrylic acid) and comparison of homogeneous and composite membrane based on polyelectrolyte complexes of Chitosan and poly(acrylic acid) for the separation of ethanol–water mixtures, J. Membr. Sci. 127 (1997) 185.
[13] D.A. Musale, S.S. Kulkarni, Effect of membrane–solute interactions on ultrafiltration performance, J. Macromol. Sci.-Rev. Macromol. Chem. Phys. 38(4), 615 (1998).
[14] A.G. Fane, C.J.D. Fell, A review of fouling and fouling control in ultrafiltration, Desalination 62 (1987) 117.
[15] D.A. Musale, S.S. Kulkarni, Fouling reduction in poly-(acrylonitrile-co-acrylamide) ultrafiltration membranes, J. Membr. Sci. 111 (1996) 49.
[16] P. Heinemann, J.A. Howell, R.A. Bryan, Microfiltration of protein solutions: effect of fouling on rejection, Desalination 68 (1988) 243.
[17] A.G. Fane, C.J.D. Fell, A.G. Waters, Ultrafiltration of protein solutions through partially permeable membranes, J. Membr. Sci. 16 (1983) 211.
[18] S. Aiba, M. Izume, N. Minoura, Y. Fujiwara, Studies on Chitin.3. Effect of coagulants and annealing on the permeation and the properties of chitin membrane, Br. Polym. J. 17 (1985) 38.
[19] W. Kaminski, Z. Modrzejewska, Application of Chitosan membranes in separation of heavy metal ions, Sep. Sci. Technol. 32(16) (1997) 2659.
[20] X. Wang, H.G. Spencer, Formation and characterization of Chitosan formed-in-place ultrafiltration membranes, J. Appl. Polym. Sci. 67 (1998) 513.
[21] M. Rinaudo, M. Milas, P.L. Dung, Characterization of Chitosan. Influence of ionic strength and degree of acetylation on chain expansion, Int. J. Biol. Macromol. 15 (1993) 281.
[22] A. Mochizuki, S. Amiya, Y. Sato, H. Ogawara, S. Yamashita, Pervaporation separation of water/ethanol mixtures through polysaccharide membranes.III. The permselectivity of the neutralized Chitosan membrane and relationships between its permselectivity and solid state structure, J. Appl. Polym. Sci. 37 (1989) 3385.
[23] G. Capannelli, F. Vigo, S. Munari, Ultrafiltration membranes: characterization methods, J. Membr. Sci. 15 (1983) 289.
[24] W.R. Bowen, R.A. Clark, Electro-osmosis at microporous membranes and the determination of zeta potential, J. Colloid Interface Sci. 97 (1984) 401.
[25] M. Oldani, G. Schock, Characterization of ultrafiltration membranes by infrared spectroscopy, ESCA and contact angle measurements, J. Membr. Sci. 43 (1989) 243.
[26] D. Murphy, M.N. de Pinho, An ATR–FTIR study of water in cellulose acetate membranes prepared by phase inversion, J. Membr. Sci. 106 (1995) 245.
[27] P.R. Griffiths, J.A. de Haseth, Fourier Transform Infrared Spectroscopy, Chemical analysis, vol. 83, Wiley, New York, 1986, p. 194.
[28] S.S. Kulkarni, E.W. Funk, N.N. Li, Membranes, in: W.S.W. Ho, K.K. Sirkar (Eds.), Membrane Handbook, Van Nostrand Reinhold, New York, 1992, pp. 409–431.